Desalination and Water Treatment
www.deswater.com

1944-3994 / 1944-3986 © 2010 Desalination Publications. All rights reserved.
doi: 10.5004/dwt.2010.1154

20 (2010) 80–85
August

Removal of oily hydrocarbon contaminants from wastewater by γ-alumina nanofiltration membranes

Z. Sadeghian[a]*, F. Zamani[b], S.N. Ashrafizadeh[b]
[a]*Gas Division, Research Institute of Petroleum Industry (RIPI), PO Box 14857-3311, West Blvd. Azadi Sport Complex, Tehran, Iran*
Tel. +98 (21) 44739551-9; Fax +98 (21) 44739716; email: sadeghianz@ripi.ir
[b]*Chemical Engineering Department, Iran University of Science and Technology (IUST),*
PO Box 16765163, Narrmak Street, Tehran, Iran

Received 8 March 2009; Accepted in revised form 24 January 2010

ABSTRACT

A supported γ-Al_2O_3 nanofiltration (NF) membrane was prepared from colloidal dispersions of bohemite via a sol–gel method. The structure and morphology of the membrane were characterized by scanning electron microscopy (SEM) and atomic force microscopy (AFM). The pore mean diameters were determined by nitrogen adsorption measurements. The filtration properties of the membrane were tested by cross flow nanofiltration using oil-in-water emulsion. The influence of the parameters such as transmembrane pressure (TMP), cross flow velocity (CFV) and oil concentration in feed were investigated by the measurements of permeate flux and total organic carbon (TOC). The removal efficiency higher than 90% was obtained under all experimental conditions.

Keywords: Alumina membrane; Nanofiltration; Oily water; Permeate flux; Cross flow

1. Introduction

Investigation of the membrane separation process for oily water treatment was started around 1973, particularly using ultrafiltration (UF) and reverse osmosis [1]. Anderson and Saw [2] investigated the effect of the modification of the membrane surface with surfactants on the performance of cross flow membrane filtration of low concentration (0.18%, v/v) emulsion of cotton seed oil-in-water, using a mixed ester asymmetric MF membrane. Scott et al. [3] reported in 1994 that they observed a total loss of rejection in the microfiltration of suspensions of decanol in water, using an MF membrane of mixed cellulose nitrate and tri-acetate. They insisted that the separation of micron or submicron emulsions would require the use of ultrafiltration membranes. Koltuniewiez et al. [4] investigated MF for the separation of oil-in-water emulsions, using three types of MF membranes. They performed simultaneous experiments in both dead-end and cross flow modes at various pressures, and in the latter case at different cross flow velocities. In the studies described above, mainly organic membranes have been used. [4–6]

Reverse osmosis and NF are useful for polishing the final effluent in wastewater treatment in large volume applications [7]. During the last decade, the interest in the use of membrane technology in general and NF in particular has emerged in wastewater treatment as well as drinking water and process water production [8]. NF has proven to be a very effective method for the removal of a wide variety of organic compounds from aqueous solution [9]. NF operations normally produce a higher water flux and can often operate at lower pressures, which reduce energy consumption in relation to reverse osmosis [10].

Ceramic NF membranes are of great interest in separation technology because of their higher chemical,

---

* Corresponding author.

thermal and mechanical stability compared to organic membranes [11].

Many studies on membrane separation for oily wastewater treatment have been reported, particularly in ultrafiltration (UF) and reverse osmosis (RO) with organic membranes [12–15]. However, few studies are related to the application of inorganic ceramic membranes on oily wastewater treatment [16]. Ceramic membranes can also be used to efficiently separate emulsions [17].

In the present study, alumina NF membranes were fabricated by the sol–gel method and applied for removal of oily hydrocarbon contaminated from wastewater.

2. Experimental

2.1. Preparation of NF membranes

Aluminum-tri-sec butylate ($[C_2H_5CH\ (CH_3)O]_3Al$) was hydrolyzed in water at 80°C (molar ratio [water]/[ASTB] = 100) and the white precipitated boehmite was maintained under vigorous agitation for 30 min. Addition of 0.12 mole of nitric acid per mole of aluminum, from an aqueous HNO_3 solution, 1.5 mol l^{-1}, allowed the peptisation of the boehmite suspension. The resulting sol was stable [19].

The supports consisted of disk-shaped with a diameter of 30 mm and a thickness of 2 mm. The supports were prepared from dry pressing of Al_2O_3 powder of high quality (>99% purity, Across Co.) at a pressure of 415 Mpa and firing at 1500°C for 2 h.

The γ-alumina nanofiltration membrane was prepared from a colloidal sol, an organic binder; the polyvinyl alcohol (12 wt% in aqueous solution) was added to the sol to adjust the viscosity. The viscous sol was then deposited for 30 min by dip coating on the former mentioned support. The membrane was then dried at room temperature during 24 h, and the gel layer was fired 2 h at the temperature of 500°C with a heating rate of 2°C /min.

Before the experiments, the membrane was immerged in ultra pure water for 18 h to obtain a stable flux at the beginning of the filtration.

2.2. Structural characterization

SEM (model VEGA/TESCAN) and AFM)Thermomicros Copes AutoProbe, USA) were used to characterize the membrane morphology, that is, the thickness and homogeneity along the support. The pore size distribution was determined from N_2 adsorption–desorption on a Micromeritics ASAP 2010 automated sorption analyzer. The Barret–Joyner–Halende (BJH) method was used to determine the pore mean size. The sample was outgassed at 300°C before the analysis.

2.3. Nanofiltration experiments

2.3.1. Sample preparation

The oil-in-water emulsion as synthetic oily wastewater was prepared by emulsifying 0.35 ml of gas oil in 1000 ml of distilled water with 0.035 ml of the surfactant, polyoxyethylene sorbitan trioleate (Tween 85), using a homogenizer (Philips) at 6000 rpm for 20 min. All the emulsions obtained were very stable. Feed concentrations of solutes were maintained approximately at 350 $mg.kg^{-1}$ in order to neglect the effect of osmotic pressure on the permeate stream.

2.3.2. Experimental set-up and operation

NF experiments were performed in cross flow equipment on a laboratory scale (Fig. 1). Flat sheet membranes with an effective membrane area of 4.5 cm^2 were used. The applied transmembrane pressure was in the range of 0.7–1.1 MPa, the cross flow velocity was between 0.56–2.8 m/s. The volume of feed solution was 20 L. The heat exchanger was used in order to keep the fluid temperature in the feed tank constant at 30±1°C. The oil-in-water emulsion was transferred from the feed tank to the NF membrane module by a centrifugal pump. The permeate sample was collected in a sample vessel and the permeate flux was measured as a function of time by weighing the permeate with an electronic balance.

2.3.3. Analytical methods

The permeate flux was continuously measured by weighing the amount of the permeation at the operation time and taking into account a filtration effective area of 4.5 cm^2. The total organic carbon (TOC) content in the feed stream and the permeate stream was determined by a total carbon analyzer (Rosemount analytical, DC-190, America). The oil hydrocarbon rejection efficiency was evaluated with the value of TOC rejection (R_{TOC}), which is defined as $R_{TOC}\ (\%) = (TOC_{feed} - TOC_{permeate}) / TOC_{feed} \times 100$.

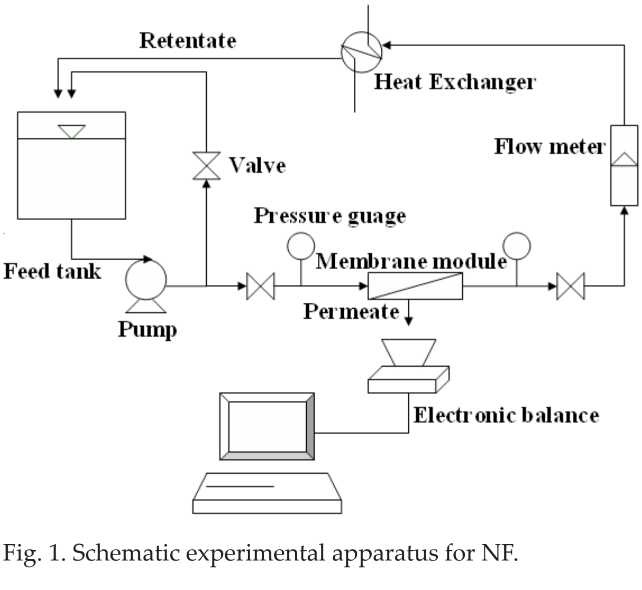

Fig. 1. Schematic experimental apparatus for NF.

3. Results

3.1. Morphology and structural characterization

Fig. 2a shows a SEM image of the top surface of the uncoated ceramic support. It can be observed that the top surface of the support contains both the macropores and mesopores. Figs. 2b and 2c present the SEM image of the top surface and cross section of γ-Al_2O_3 layer deposited on the support, respectively. It can be observed from Fig. 3b that the top layer contains nanopores. By looking at Fig. 2c, an average thickness of 1.5 μm can be estimated for the γ-Al_2O_3 layer deposited on the support.

Also, as shown by the AFM image (Fig. 2d), it confirms the smooth appearance of the top layer made by the sol–gel procedure. Therefore, it is apparent that a relatively thin and a very homogeneous membrane top layer were formed.

Figs. 3a and 3b show the pore size distribution measured of N_2 adsorption–desorption isotherms for the samples of the support and the formed γ-Al_2O_3 layer. The results show that the distribution of the pore size at the support and γ-Al_2O_3 layer is very sharp and concentrated at 22 nm and 0.99 nm, respectively.

3.2. Filtration tests

3.2.1. Pure water and oily wastewater permeation measurement

Fig. 4 shows the time dependency of the permeation flux measured with the samples of distilled water and oily water. The temperature was controlled at 30°C. The working pressure was 5 bar. The cross flow velocity filtration loop was 1.12 m/s. Each test operated 1.2 h in order to obtain the steady state pure water flux. The value of total organic carbon (TOC) in the sample of oily water was maintained at 260 $mg.kg^{-1}$.

As shown as in Fig. 4, the water permeation flux in pure water varies constantly with time, but the water permeation flux in the sample of oily water decreases obviously for the early filtration time and gradually reaches a constant value due to a fouling consolidation (concentration polarization, gel layer and cake layer) caused by the presence of the solute.

3.2.2. Effects of transmembrane pressure on flux

Increasing pressure increases permeation flux, but at the same time causes the cake layer on the membrane

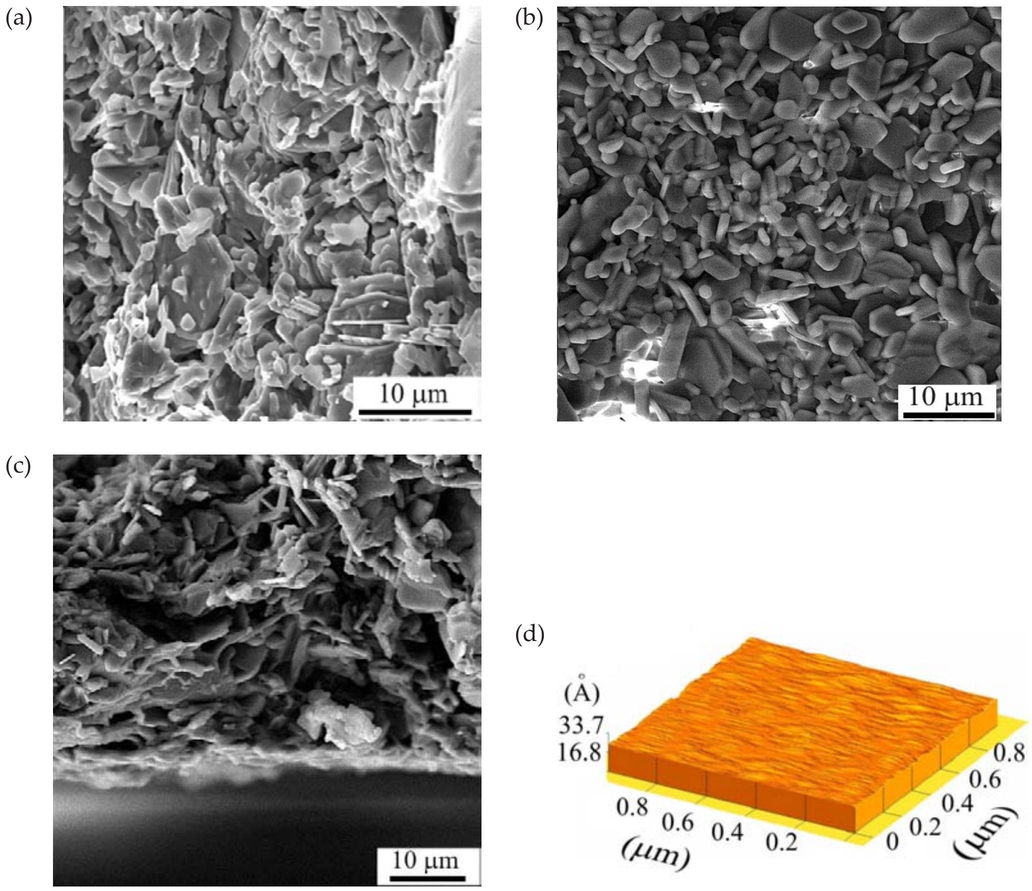

Fig. 2. SEM images of (a) top surface of uncoated ceramic support: (b) top surface of γ-alumina layer (c) cross-section of γ-alumina layer and (d) AFM image of γ-alumina layer.

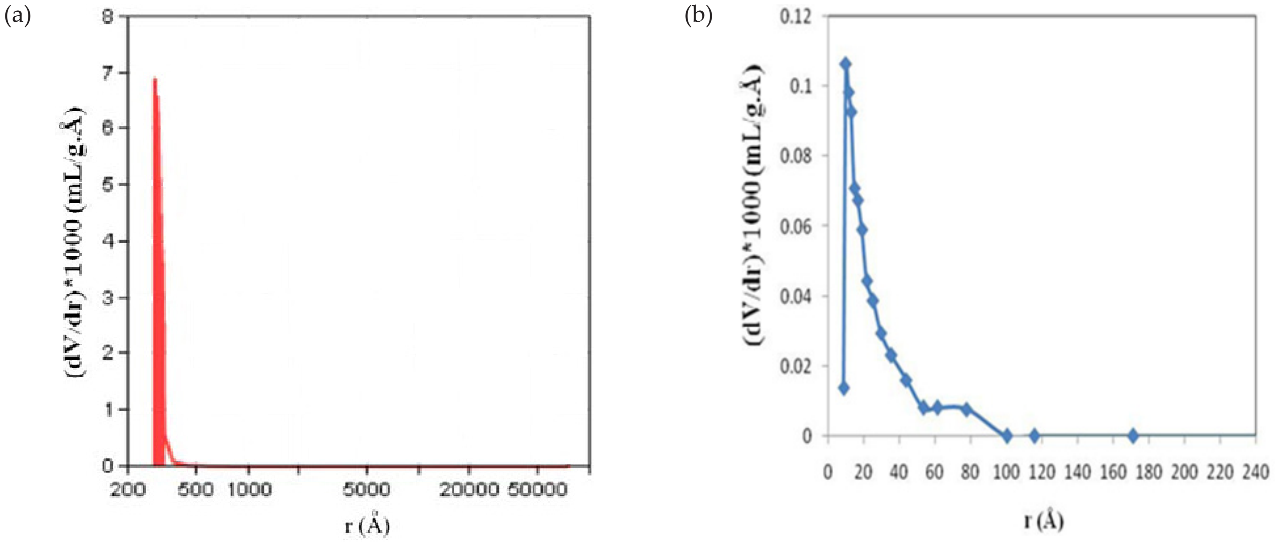

Fig. 3. Pore size distribution of NF alumina membrane surface of (a) uncoated ceramic support (b) top surface of γ-alumina layer.

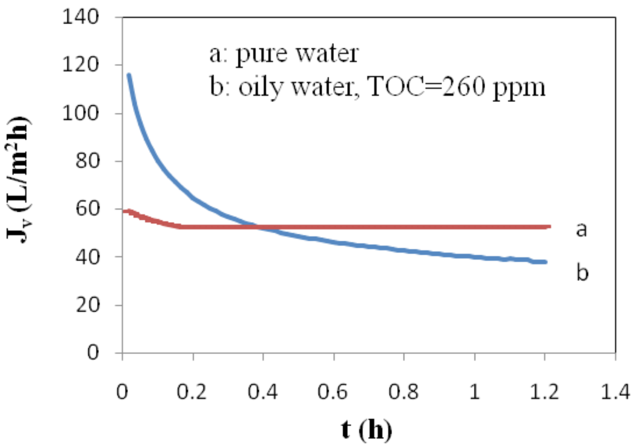

Fig. 4. Water permeation flux as function of time for (a) pure water and (b) oily water.

surface to compress [20,21]. Fig.5 shows the effect of transmembrane pressure which was adjusted to varying with 0.7, 0.8, 0.9, 1 and 1.1 MPa respectively on the permeation flux.

With increasing the pressure, TOC concentration in permeate rises lead to reduction of permeate quality. The flux of stable state is also significantly higher under the higher transmembrane pressure. This can be explained that the higher transmembrane pressure results in droplets (both solvents and solute) to pass rapidly through the membrane pores. The oil hydrocarbons droplets may be deformed partially to cause oil compaction under the higher transmembrane pressure. Therefore, the TOC concentration in the permeation was a bit higher under higher pressure [21].

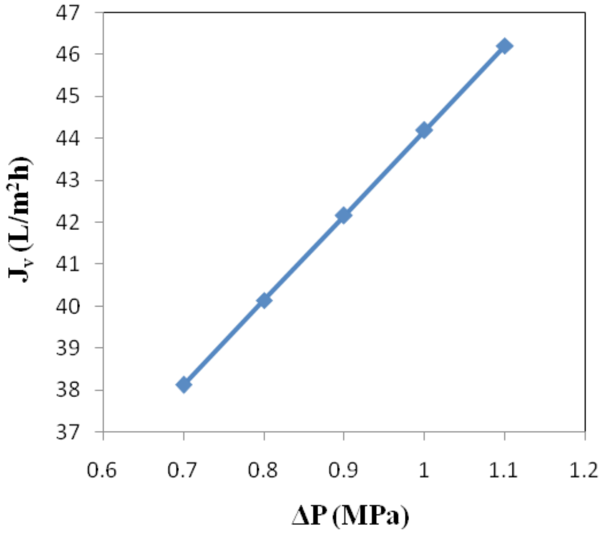

Fig. 5. The effect of transmembrane pressure on permeation flux.

3.2.3. Effects of cross flow velocity on permeation flux

Fig. 6 shows the effect of cross flow velocity adjusted to 0.56, 1.12, 1.68, 2.23 and 2.8 m/s respectively on the permeation flux. The steady state permeate flux rises when the cross flow velocity increases. Low cross flow velocity results in obvious resistance of concentration polarization and the gel layer. Turbulency and shear stress on the membrane surface increase at the higher cross flow velocities. Accumulation of solute on the membrane surface is then easily retained to the bulk, and the effect of concentration polarization diminishes. Thus, the per-

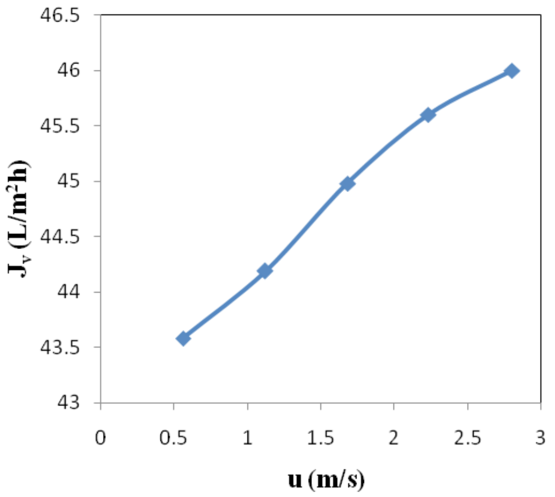

Fig. 6. The effect of cross flow velocity on permeation flux.

meation flux increases with increasing cross flow velocity [21]. In these experimental conditions, with the increase in the permeate flux; a little difference happened in the levels (%) of TOC rejection.

3.2.4. Effect of oil hydrocarbons concentration (TOC concentration) on permeation flux

Increasing concentration decreases the effective pressure difference and subsequently the permeation flux. Fig. 7 shows the dependence of the permeation flux with varying oil hydrocarbons concentrations (TOC concentration) between 260–80 mg.kg^{-1}. Obviously, the permeation flux decreases for all variable concentrations of TOC. High flux at lower oil hydrocarbons concentrations can be explained by the insufficient formation of the oil layer on the membrane, which results in low percentages of the cake layer resistance. Increasing the concentration causes the layer formed on the membrane surface to be thick and significant concentration polarization. As an increase of oil hydrocarbons concentration was applied, the flux decreased obviously and the TOC in the permeation increased significantly. Both facts are because the cake layer resistance and the passage of oil droplets through the membrane pores increased. That resulted from the increase of the oil layer on the membrane [21].

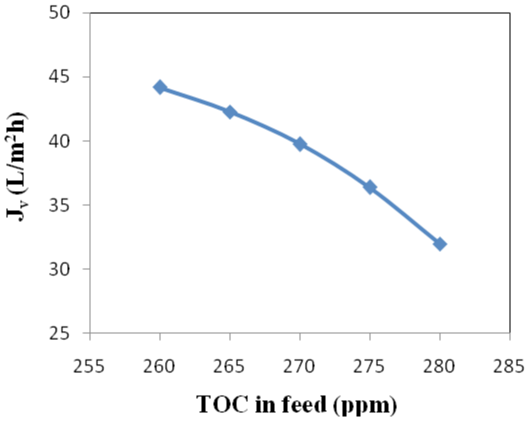

Fig. 7. Effect of TOC concentration in feed on permeation flux.

3.2.5. TOC rejection

Table 1 shows the TOC rejection efficiencies at the steady state for various runs. Under applied operational conditions, TOC rejection efficiencies remained at a high level and were always higher than 90%.

4. Conclusion

The experimental results indicate that the ceramic NF membrane can be applied to provide a high relative flux and a high oil hydrocarbons removal efficiency. The permeation flux was increased under these conditions, such as raising transmembrane pressure, increased cross flow velocity and reducing the oil concentration in the feed solution. TOC rejection efficiencies with various operational conditions were as high as 90% or above.

References

[1] R.L. Goldsmith and S. Hossain, Oil water separation by ultrafiltration, Proc. Joint Conference on Prevention and Control of Oil Spills, 1973, pp. 441–456.
[2] G.K. Anderson and C.B. Saw, Oil/water separation with surface modified membranes, Environ. Tech. Lett., 8 (1987) 121–132.
[3] K. Scott, A. Adhamy, W. Atteck and C. Davidson, Crossflow microfiltration of organic/water suspensions, Wat. Res., 28(1) (1994) 137–145.
[4] A.B. Koltuniewicz, R.W. Field and T.C. Arnot, Cross-flow and

Table 1
TOC concentration and rejection efficiency

Pressure (MPa)	0.8	0.9	1	1	1	1	1	1	1
Velocity (m/s)	1.12	1.12	1.12	1.12	1.12	1.12	1.12	1.68	2.23
Oil concentration (mg/L)	260	260	260	260	270	280	260	260	260
TOC permeate (mg/L)	9.1	9.62	10.4	10.4	24.3	30.8	9.1	9.62	9.88
TOC rejection efficiency (%)	96.5	96.3	96	96	91	89	96.5	96.3	96.2

dead-end microfiltration of oily-water emulsion. Part 1: Experimental study and analysis of flux decline, J. Membr. Sci., 102 (1995) 193–207.

[5] P. Gallagher, Membrane removal processes for oil-water emulsion treatment, Water Waste Treat., August (1992) 42–43.

[6] R.R. Bhave, J. Guibaud and R. Rumeau, Inorganic membranes for the filtration of water, wastewater treatment and process industry filtration applications, R.R. Bhave, ed., Inorganic Membranes, New York, 1991, pp. 275–299.

[7] H. Ohya, J. J. Kim, A. Chinen, M. Aihara, S. I. Semenova, Y. Negishi, O. Mori and M. Yasuda, Effects of pore size on separation mechanisms of microfiltration of oily water, using porous glass tubular membrane, J. Membr. Sci., 145 (1998) 1–14

[8] B. Van der Bruggen, M. Mänttäri and M. Nyström, Drawbacks of applying nanofiltration and how to avoid them: A review, Sep. Purif. Technol., 63 (2008) 251–263.

[9] P. Berg, G. Hagmeyer and R. Gimbel, Removal of pesticides and other micropollutants by nanofiltration, Desalination, 113 (1997) 205–208.

[10] R. Haddad, E. Ferjani, M.S. Roudesli and A. Deratani, Properties of cellulose acetate nanofiltration membranes. Application to brackish water desalination, Desalination 167 (2004) 403–409.

[11] S. Benfer, U. Popp, H. Richter, C. Siewert and G. Tomandl, Development and characterization of ceramic nanofiltration membranes, Sep. and pur. Technol., 22–23 (2001) 231–237.

[12] S. Lee, Y. Aurelle and H. Roques, Concentration polarization, membrane fouling and cleaning in ultrafiltration of soluble oil, J. Membr. Sci., 19 (1984) 23–38.

[13] B.H. Chiang and M. Cheryan, Modelling of hollow-fibre ultrafiltration of skimmilk under mass-transfer limiting conditions, J. Food Eng., 6 (1987) 241–255.

[14] P. Lipp, C.H. Lee, A.G. Fang and C.J.D. Fell, A fundamental study of the ultrafiltration of oil–water emulsions, J. Membr. Sci., 36 (1988) 161–177.

[15] J. Cho, G. Amy and J. Pellegrino, Membrane filtration of natural organic matter: factors and mechanisms affecting removal efficiency and flux decline with charged ultrafiltration (UF) membrane, J. Membr. Sci., 164 (2000) 89–110.

[16] F.L. Hua, Y.F. Tsang, Y.J. Wang, S.Y. Chan, H. Chua and S.N. Sin, Performance study of ceramic microfiltration membrane for oily wastewater treatment, Chem. Eng. J., 128 (2007) 169–175.

[17] S.R. Fontes, V.M.S. Queiroz, E. Longo and M.V. Antunes, Tubular microporous alumina structure for demulsifying vegetable oil/water emulsions and concentrating macromolecular suspensions, Sep. Purif. Technol., 44 (2005) 235–241.

[18] S.R. Fontes, E. Longob and R. Del Colle, Demulsification of water/sunflower oil emulsions by a tangential filtration process using chemically impregnated ceramic tubes, J. Membr. Sci., 289 (2007) 58–66.

[19] A. Larbot, S. Alami Younssi, M. Persin, J. Sarrazin and L. Cot, Preparation of a γ-alumina nanofiltration membrane, J. Membr. Sci., 97 (1994) 167.

[20] T. Mohammadi and A. Esmaeelifar, Wastewater treatment using ultrafiltration at a vegetable oil factory, Desalination, 166 (2004) 329–337.

[21] F.L. Hua, H. Chua, Y.J. Wang, S.Y. Chan and Y.F. Tsang, Oily wastewater treatment by means of ceramic membrane, Proc. 2nd IASTED International conference, 2006, pp. 112–117.